

**THE MAPPING X-RAY FLUORESCENCE SPECTROMETER (MAPX).** David Blake<sup>1</sup>, Philippe Sarrazin<sup>2</sup>, Thomas Bristow<sup>1</sup>, Robert Downs<sup>3</sup>, Marc Gailhanou<sup>4</sup>, Franck Marchis<sup>2</sup>, Douglas Ming<sup>5</sup>, Richard Morris<sup>5</sup>, Vicente Armando Solé<sup>6</sup>, Kathleen Thompson<sup>2</sup>, Philippe Walter<sup>7</sup>, Michael Wilson<sup>1</sup>, Albert Yen<sup>8</sup> and Samuel Webb<sup>9</sup>, <sup>1</sup>NASA Ames Research Center, Moffett Field, CA - david.blake@nasa.gov, <sup>2</sup>SETI Institute, Mountain View, CA, <sup>3</sup>Univ. of Arizona, Tucson AZ, <sup>4</sup>IM2NP, Université Paul Cézanne, Marseille, France, <sup>5</sup>NASA Johnson Space Center, Houston, TX, <sup>6</sup>ESRF, Grenoble, Fr, <sup>7</sup>Université Pierre et Marie Curie, Paris, Fr., <sup>8</sup>JPL, Pasadena, CA, <sup>9</sup>SLAC, Stanford, CA.

**Introduction:** Many planetary surface processes leave traces of their actions as features in the size range 10s to 100s of  $\mu\text{m}$ . The Mapping X-ray Fluorescence Spectrometer (MapX) will provide elemental imaging at  $\leq 100\mu\text{m}$  spatial resolution, yielding elemental chemistry at a scale where many relict physical, chemical, or biological features can be imaged and interpreted in ancient rocks on Mars or on the surfaces of other planetary bodies/planetesimals.

**MapX:** MapX is an arm-based instrument positioned on soil or regolith with touch sensors. During an analysis, an X-ray source (tube or radioisotope) bombards the sample with X-rays or  $\alpha$ -particles /  $\gamma$ -rays, resulting in sample X-ray Fluorescence (XRF). X-rays emitted in the direction of an X-ray sensitive CCD imager pass through a 1:1 focusing lens (X-ray  $\mu$ -pore Optic (MPO)) that projects a spatially resolved image of the X-rays onto the CCD. The CCD is operated in single photon counting mode so that the energies and positions of individual X-ray photons are recorded. In a single analysis, several thousand frames are both stored and processed in real-time. The MapX concept is illustrated in Fig. 1.

Higher level data products include single-element maps with a lateral spatial resolution of  $\leq 100\mu\text{m}$  and quantitative XRF spectra from ground- or instrument-selected Regions of Interest (ROI). XRF spectra from ROI are compared with known rock and mineral compositions to extrapolate the data to rock types and putative mineralogies.

**Proof of concept prototypes:** Earlier prototypes [1-3] demonstrated proof-of-concept using COTS components. MapX-II (Fig. 2) utilizes an Andor iKon M camera with 1024x1024 back illuminated deep depletion CCD. Two 40kV-4W Au target transmission window X-ray tubes (Moxtek) illuminate the sample. An MPO X-ray focusing lens (PHOTONIS) is placed equidistant between the sample location and the CCD. The lens derives from “lobster-eye” multichannel optics used for X-ray astronomy [4]. It is implemented here in a flat geometry for 1:1 focusing. This lens provides a much improved aperture when compared to pin-hole camera optics having similar spatial resolution, and true focusing when compared to polycapillary collimating optics also used for X-ray mapping. The camera is driven at up to 3 frames per second, and the X-ray sources are shuttered during read cycles.

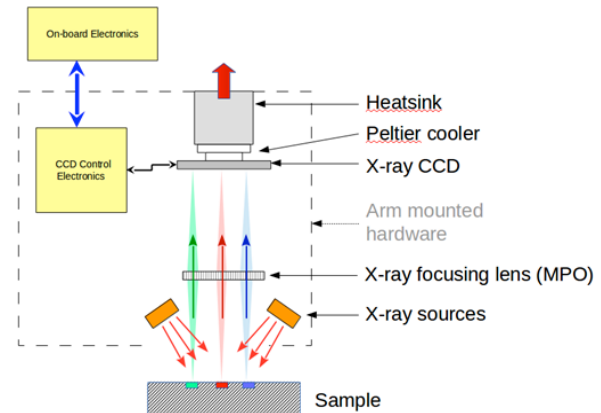


Fig. 1: Schematic drawing of the MapX concept.

#### Other work in progress:

**Development of data processing software.** The instrument collects a large number of short acquisitions that are combined into X-Y-time data cubes. Python code was developed for processing raw CCD data from the prototypes. This code includes background correction, split charge removal and optional binning features. The resulting X-Y-energy data cubes are stored in HDF5 format and quantified with PyMca [5] using fundamental parameters methods.

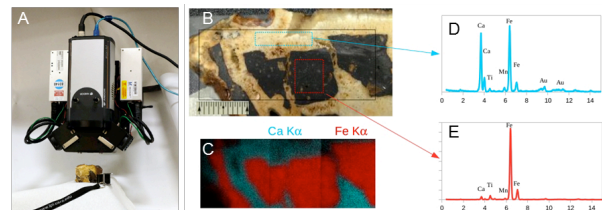


Fig. 2. MapX-II Prototype. A) MapX-II in position to analyze a rock sample. B) Optical image of sample composed of basalt fragments and light-toned cement (scale in mm). C) FeK $\alpha$ /CaK $\alpha$  map obtained by tiling 3 analyses of 1000s integration. D-E) XRF spectra of ROI chosen from the MapX-II image shown in “C.”

**Characterization and correction of the MPO Point Spread Function (PSF).** The MPO lens causes a signal spread on the detector that must be corrected for optimum spatial resolution. The PSF varies with photon energy and with X-Y position due to morphological or stacking defects of the micro-channels. Experiments are being performed at the Stanford SSRL to character-

ize the PSF, and ray-tracing models of the MPO have been developed in parallel to evaluate the effects of various types of defects on the PSF and to assist in the development of PSF deconvolution algorithms [6] (e.g., Fig. 3). Figure 4 shows results in which a deconvolution algorithm based on an observed PSF was applied to data from an imaging standard.

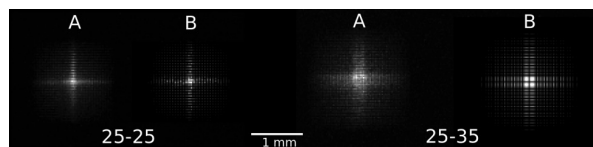


Fig. 3. Comparison of MPO PSF data (A) collected at SSRL BL2-3 and (B) obtained by ray tracing simulations at a nominal CCD-MPO distance of 25mm. Left: sample in focus (25-25); Right: sample out of focus by 10mm (25-35). A 10 mm defocus condition results in a point resolution decrease of  $\sim 100 \mu\text{m}$ .

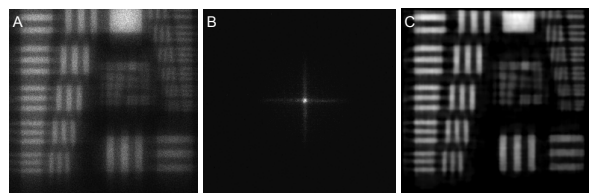


Fig. 4. MapX PSF Deconvolution Example (1951 USAF resolution standard, Cr on glass). A) Original image. CrK $\alpha$ , taken with MapX-II (MPO-CCD, MPO-Target = 50 mm). The resolution of this image is estimated to be  $200 \mu\text{m}$ . B) Measured PSF from the SLAC experiment (FWHM  $\sim 165 \mu\text{m}$ ). C) AIDA [6] deconvolution with automatized cost function parameters (resolution  $\sim 160 \mu\text{m}$ ).

**X-ray and  $\gamma$ -ray/ $\alpha$ -particle radioisotope source requirements.** Source requirements for MapX are determined through Monte Carlo modeling and experiment. XMIMSIM [7], GEANT4 [8] and PyMca [5] are being used along with a dedicated XRF test fixture to determine detection limits and accuracy/precision for elements of interest. Preliminary results indicate that either a 3W X-ray tube source, or a 30mCi  $^{244}\text{Cm}$  radioisotope source (as carried on the APXS instruments) will be sufficient to meet MapX science objectives.

**Development of high-TRL MapX components.** In parallel with method development and laboratory and field prototype refinement, engineering efforts are being pursued to increase the TRL of the instrument. MapX-III (Fig. 5) is being built with a CCD224 imager (MSL CheMin heritage) driven by dedicated CCD electronics using flight design standards. The new camera prototype will demonstrate the basic architecture of a flight camera for an arm mounted instrument and will serve as a base for an in-vacuum MapX prototype to characterize the system capabilities at the low

X-ray energies (e.g., K $\alpha$  lines for Na) that are absorbed in the in-air current prototypes.

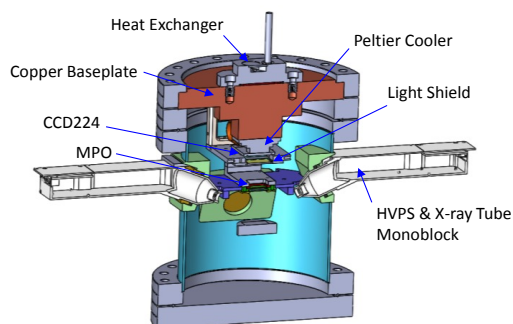


Fig. 5. TRL-4 MapX-III prototype with X-ray tube sources, MSL CheMin heritage CCD224 CCD package, exchangeable MPO and modifiable geometry.

**Flight instrument concept:** Fig. 6 shows a conceptual illustration of an arm-deployed MapX instrument (with X-ray tube sources). Replacing X-ray sources with radioisotope sources would reduce the mass by 1 kg. and the power by 10W. Not shown is a Rover Avionics Mounting Platform (RAMP) unit that houses the Control and Processing Electronics (CPE).

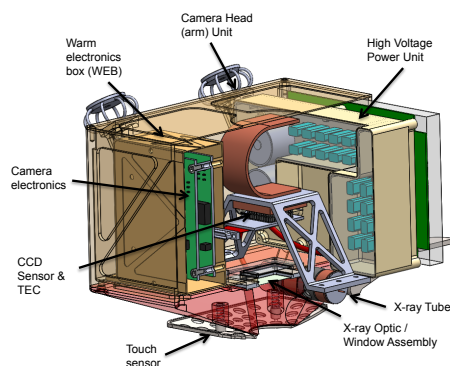


Fig. 6. Notional Flight configuration of MapX Arm Unit (X-ray Tube version) enclosing the Camera Head Electronics (CPE).

**References:** [1] D.F. Blake et al. (2014) IPM-2014, #1080. [2] D.F. Blake et al. (2015) LPSC XLVI #2274. [3] P. Sarrazin et al. (2016) LPSC XLVII #2883. [4] G. W. Fraser et al. (2010) Planet. Space Sci. 58 (1-2), 79–95. [5] V.A. Solé, et al. (2007) Spectrochim. Acta B 62 63–68. [6] Hom, E.F.Y. et al. (2007) J. Opt. Soc. of America. A, 24(6), pp. 580–600. [7] Schoonjans T. et al. (2012) Spectrochim. Acta Part B, 70, 10–23. [8] Agostinelli, S. et al. (2003) Nucl. Instr. and Methods in Phys. Res. A, 506, 250–303.

**Acknowledgements:** DB is grateful for support from NASA/ARC's Center Innovation Fund and NASA's PICASSO program (grant # NNX14AI28A).